

Contrasting effects of phase-oriented antioxidant localization on oxidative resistance and physical stability of double emulsions

Received: 27 June 2025

Accepted: 6 January 2026

Cite this article as: Jeon, S., Jeong, J., Sumnu, G. *et al.* Contrasting effects of phase-oriented antioxidant localization on oxidative resistance and physical stability of double emulsions. *npj Sci Food* (2026). <https://doi.org/10.1038/s41538-026-00716-8>

Seungtak Jeon, Jaehyun Jeong, Gulum Sumnu, Serpil Sahin, Mi-Jung Choi & Jiseon Lee

We are providing an unedited version of this manuscript to give early access to its findings. Before final publication, the manuscript will undergo further editing. Please note there may be errors present which affect the content, and all legal disclaimers apply.

If this paper is publishing under a Transparent Peer Review model then Peer Review reports will publish with the final article.

Contrasting Effects of Phase-Oriented Antioxidant Localization on Oxidative Resistance and Physical Stability of Double Emulsions

Seungtak Jeon^a, Jaehyun Jeong^a, Gulum Sumnu^b, Serpil Sahin^b, Mi-Jung Choi^c & Jiseon Lee^{c,*}

^aDepartment of Food Science and Biotechnology of Animal Resources, Konkuk University, 05029, Seoul, Korea

^bDepartment of Food Engineering, Middle East Technical University, 06800, Ankara, Turkey

^cSchool of Animal, Food Science and Marketing, Konkuk University, 05029, Seoul, Korea

***Corresponding author: Jiseon Lee**

Email: jmango021@konkuk.ac.kr

Abstract

This study investigated the effect of functional antioxidant incorporation and spatial localization on physicochemical and oxidative stability of water-in-oil-in-water ($W_1/O/W_2$) double emulsions. Paprika oleoresin (PO, lipophilic) in the oil phase and gallic acid (GA, hydrophilic) in the inner (W_1), outer (W_2), and aqueous phases were studied. The effects of antioxidant localization on droplet size, viscosity, ζ -potential, encapsulation efficiency, and oxidative stability were evaluated over four weeks of storage. PO reduced interfacial tension by ~10%, leading to smaller droplets (2.6–2.5 mN/m) and improved oxidative stability. GA in the W_2 phase enhanced radical-scavenging activity (DPPH and ABTS assays) by >30% compared to the control, but decreased ζ -potential (from -32 to -26 mV) and viscosity, leading to increased creaming ($\leq 19\%$). Dual GA incorporation (W_1 and W_2) showed the highest overall antioxidant capacity but also accelerated pH decline and structural deterioration. These results demonstrate that antioxidant distribution determines destabilization mechanisms in complex emulsions, and phase-oriented interfacial design is essential to balance oxidative protection and structural integrity in multiphase food systems.

Keywords: Paprika oleoresin; Gallic acid; Stability; Antioxidant partitioning; $W_1/O/W_2$ emulsion system; Interfacial structure

Introduction

Water-in-oil-in-water ($W_1/O/W_2$) double emulsions are multiphase systems of colloidal dispersions in which water-in-oil (W/O) emulsions are dispersed as globules within an external aqueous phase^{1,2}. Double emulsions offer several distinctive advantages, including controlled release of encapsulated hydrophilic and lipophilic bioactive compounds, protection of sensitive components, and masking of undesirable flavors in inner-phase substances³. These properties make double emulsions an attractive delivery system for bioactive compounds.

Despite these advantages, double emulsions are susceptible to chemical instability, particularly lipid oxidation. The high specific surface area between the oil and aqueous phases can accelerate lipid oxidation, resulting in the formation of harmful compounds, off-odors, and decreased emulsion stability¹. To prevent such oxidative deterioration, incorporating antioxidants such as gallic acid (GA) and paprika oleoresin (PO) is recommended, as they effectively scavenge free radicals and chelate prooxidant metal ions⁴.

Antioxidants positively affect chemical stability, but also present challenges to physical stability. The addition of antioxidants can influence interfacial properties at both the water-in-oil and oil-in-water interfaces, potentially inducing physical instability. This phenomenon can result in droplet coalescence, Ostwald ripening, inner droplets swelling or shrinkage, and molecular diffusion between the phases^{1,3,5,6}. Additionally, the greater interfacial area between oil and water in double emulsions increases their susceptibility to lipid oxidation compared with single emulsions⁷. Therefore, both chemical and physical instabilities should be carefully considered during formulation, with particular focus on lipid oxidation as the primary destabilizing factor. Various strategies have been developed to improve the physicochemical stability of complex emulsion systems through structural reinforcement and interfacial modifications. For instance, protein-based complexes have been utilized to strengthen the network of high internal phase emulsions, leading to improved physical integrity and functional

properties⁸. Similarly, a combination of physical and enzymatic treatments has been reported to regulate interfacial behavior and enhance overall emulsion stability⁹. Hwang et al.⁵ reported that incorporating soybean protein isolate, gallic acid, and xanthan gum effectively stabilized high internal phase double emulsions, emphasizing the synergistic role of protein–polyphenol–polysaccharide interactions in improving interfacial stability and encapsulation performance. These approaches highlight the importance of interfacial control in stabilizing multiphase emulsions. However, the specific effects of antioxidant phase localization on the interfacial characteristics and stability of double emulsions remain insufficiently understood.

Stabilizing double emulsions under oxidative and physicochemical stresses remains a major challenge. Incorporating both hydrophilic (GA) and lipophilic (PO) antioxidants is a promising approach for improving overall stability. However, despite extensive studies on antioxidant-enriched emulsions, the influence of antioxidant phase localization on interfacial behavior and overall stability remains poorly understood. Addressing this gap is essential for the development of phase-specific stabilization strategies with practical relevance to high-viscosity food systems.

Therefore, this study aimed to examine the effects of GA localization (inner aqueous phase W_1 , outer aqueous phase W_2 , or both phases) and PO addition (to the oil phase) on the physicochemical properties and oxidative stability of $W_1/O/W_2$ double emulsions with a high internal phase ratio. It is hypothesized that the localization of GA within different aqueous phases will alter interfacial organization and antioxidant distribution, thereby affecting the overall structural stability and oxidative resistance of the emulsions. These findings are expected to provide insights into the design of structurally stable emulsion systems applicable to high-viscosity food products such as sauces, dressings, and functional spreads.

Results and discussion

Interfacial tension

Interfacial tension is defined as the force required to expand the interface between two immiscible liquids¹. In double emulsions, they stabilize dispersed droplets and prevent coalescence. Table 1 presents the interfacial tension values between the aqueous and oil phases, which indicate the influence of GA and PO on the interfacial properties of the emulsion. The addition of 0.5% GA to the aqueous phase significantly reduced interfacial tension compared to the control (0%), which can be attributed to its amphiphilic nature, possessing both hydrophilic and hydrophobic groups¹⁰. As a result, GA can be adsorbed at the water-oil interface and lowers the interfacial tension. Organic acids, such as GA act as cosurfactants or cosolvents, modifying both the aqueous phase and interfacial region¹¹, thereby enhancing emulsification and potentially improving long-term stability.

Similarly, the incorporation of PO decreased the interfacial tension. At the W_1/O interface, it dropped from 2.6–2.8 to 2.5–2.6 mN/m, and at the O/W_2 interface, from 1.0 to 0.7–0.9 mN/m (Table 1). PO contains carotenoids such as capsanthin, capsorubin, and zeaxanthin, which exhibit both antioxidant and interfacial activities. Li et al.¹² reported that capsanthin adsorbs at the oil/water interface, forming a compact interfacial membrane that reduces interfacial tension and increases surface pressure, thus improving emulsion stability. The presence of these lipophilic antioxidants in the oil phase likely facilitates interfacial interactions, further stabilizing the emulsion.

The synergistic reduction in interfacial tension through dual antioxidant localization highlights the potential for tailoring interfacial characteristics to improve emulsion stability in complex multiphase food systems. This may result from antioxidant partitioning between phases, enhancing interfacial adsorption and reinforcing droplet structure. Since a lower interfacial tension promotes emulsification and limits coalescence, these findings indicate that both GA and PO contribute to emulsion stability by modifying interfacial characteristics¹¹.

However, further studies are required to assess long-term effects on droplet size, coalescence, and physicochemical stability.

Morphology and droplet size

Morphology and droplet size of $W_1/O/W_2$ double emulsions are shown in Fig. 1 and 2A, respectively. All double emulsions successfully formed a distinct internal aqueous phase encapsulated within oil droplets, as confirmed by optical microscopy and confocal laser scanning microscopy (CLSM) images (Fig. 1). The CLSM images further support these results, clearly showing the internal aqueous phase encapsulated within oil phase, thus verifying the successful formation of a double emulsion structure. In addition to the micrographs of fresh emulsions presented in Fig. 1, optical microscopy was also employed to monitor the morphological features of the double emulsions during storage. The images obtained after 0, 1, 2, and 4 weeks are provided in Fig. S1.

In the fresh state, double emulsions with 0.5% PO in the oil phase exhibited significantly smaller droplet sizes compared to the control (canola oil, CO, in the oil phase). This decrease in droplet size can be attributed to the reduction in interfacial tension facilitated by PO under constant homogenization conditions (Table 1)¹³. Additionally, the incorporation of GA significantly reduced the droplet sizes of both the PO and CO double emulsions. The particle size of the fresh double emulsions decreased in the following order: NN, NG, GN, and GG (Fig. 2A). The amphiphilic nature of GA, which allows adsorption at the oil-water interface, further reduces the interfacial tension, facilitating the formation of smaller droplets. Disruption during homogenization leads to smaller droplet sizes⁵. The smaller droplet size resulting from the addition of GA reduces the terminal droplet velocity according to Stokes' law, thereby improving the physical stability of the emulsion during storage¹⁴. These results also indicate that the localization of antioxidants critically influences droplet size; specifically, positioning

GA in the external aqueous phase (NG and GG) resulted in smaller droplets compared to its placement in the internal aqueous phase alone (GN). However, it is noteworthy that smaller droplet sizes, which are beneficial for reducing sedimentation and improving emulsion stability, may also increase susceptibility to Ostwald ripening. The instability of PO emulsions can also be explained by diffusion-driven processes. According to Rao and McClements¹³, essential oils containing moderately water-soluble terpenes are prone to Ostwald ripening because these molecules preferentially diffuse into the aqueous phase. Given that PO contains terpenoid compounds with comparable solubility characteristics, such diffusion-induced redistribution may have contributed to the accelerated creaming and droplet growth observed in PO emulsions.

Color value

Table 2 shows the color changes of the double emulsion during storage. The CO double emulsion without PO exhibited higher L^* values than the PO double emulsion but lower a^* and b^* values. Fig. 2B shows the calculated whiteness values of the emulsions. Initially, smaller droplet sizes enhanced the whiteness owing to increased light scattering¹⁵. However, during storage, aggregation and phase separation resulted in a decline in whiteness, which was particularly noticeable in the PO emulsions. Additionally, the inclusion of GA significantly reduced the whiteness value, likely due to its effect on decreasing droplet size, thereby enhancing light absorption and reducing overall light scattering within the emulsion system. The whiteness values decreased in the order of NN, NG, GN, and GG, aligning well with the droplet size results (Fig. 2A). Incorporating GA negatively affected the physical stability of the double emulsion.

Furthermore, the PO double emulsion showed a significant increase in a^* and b^* values over the storage period. Chantrapornchai et al.¹⁶ reported that dye-containing emulsions exhibit

enhanced chromatic intensity, resulting in elevated a^* and b^* values at equivalent dispersed oil concentrations. According to these authors, this phenomenon occurs because, as the droplet size increases beyond 0.5 μm , the scattering efficiency of the droplets decreases, allowing light to penetrate the emulsion, thereby enhancing dye absorption.

Creaming index

The appearance and creaming index (CI) of the double emulsion, influenced by varying compositions of W_1 , W_2 , and O phases, are shown in Fig. 3A and B, respectively. Initially, no separation was observed in the fresh double emulsion (Fig. 3A). However, during the four-week storage period, the CI increased significantly in samples containing GA ($p < 0.05$). The CI of the PO double emulsion ranged from approximately 9–19%, which was higher than that of the CO double emulsion, ranging from about 0–14%. No oiling-off, which is attributed to oil droplet coalescence, was observed in the emulsions after up to two weeks of storage. This stability is primarily due to the steric repulsion imparted by Tween® 80, a non-ionic surfactant with a high hydrophile-lipophile balance (HLB), used as the emulsifier in the W_2 phase. According to Wu et al.¹⁷, Tween® 80 effectively stabilizes by forming a protective layer around oil droplets, thus preventing their coalescence. It maintains emulsion stability under challenging conditions, such as low pH, high ion concentration, and elevated temperatures. Doost et al.¹⁸ further affirm that the high HLB value of Tween® 80 enhances its ability to ensure long-term stability of the emulsion.

Nonetheless, after four weeks, a slight oiling-off was noted at the surface region of the GG and NG samples (Fig. 3A), indicating that the addition of PO adversely affected the physical stability of the high internal phase double emulsions. Smaller droplet size in PO emulsions leads to increased surface area exposure. Combined with the high polarity of flavor oils, such as orange and lemon oils, this results in reduced viscosity and increased susceptibility

to Ostwald ripening, ultimately diminishing the stability of the emulsion. Saari and Chua¹⁹ and Lee et al.¹ report similar findings, with flavor oils exhibiting low viscosity and high-water solubility, making them susceptible to Ostwald ripening. Additionally, de Aguiar et al.²⁰ noted that PO emulsions made with modified starch exhibited a uniform droplet size, which is a hallmark of Ostwald ripening.

ζ-potential

Fig. 3C shows the ζ-potential of the double emulsions. All emulsions exhibited a negatively charged ζ-potential, indicating the presence of electrostatic repulsive forces. The addition of electrolytes to the continuous phase increased the absolute ζ-potential value, enhancing droplet stability through greater electrostatic repulsion^{6,21}. Typically, emulsions with an absolute value of ζ-potential above 30 mV are considered electrostatically stable²¹. However, PO emulsions exhibited smaller ζ-potential values compared to CO emulsions, although all except for PO-NG registered higher than -30 mV. This variance could be due to the different charge characteristics of the oil mixture components and bioactive elements²². Notably, the addition of lipophilic antioxidants, such as α-tocopherol, to flaxseed oil-based emulsions has been shown to reduce the ζ-potential. Additionally, Losada-Barreiro et al.²³ found that increasing the hydrophilic-lipophilic balance of non-ionic surfactants shifted the distribution of these antioxidants from the oil phase to the interfacial region, affecting the ζ-potential. Capsanthin, capsorubin, and tocopherol in PO likely contributed to the reduced ζ-potential in PO emulsions²⁴. In addition, this reduction could be related to the interfacial participation of carotenoid molecules. Previous studies have shown that carotenoids and oleoresin components can integrate into the interfacial layer together with emulsifiers, potentially altering its compactness and charge distribution²⁵.

The addition of GA influenced the ζ -potential differently depending on its location in the double emulsion. GN displayed a ζ -potential similar to NN, NG increased, and GG decreased. GA can acquire a negative charge upon dissociation, potentially expanding the ζ -potential when added to the external aqueous phase^{11,26}. However, in W/O emulsions, GA at the oil-water interface might reduce the electrostatic repulsion between water droplets caused by NaCl dissociation during homogenization¹¹. This effect likely explains the observed ζ -potential changes in the NG, GN, and GG formulations. Moreover, de Moaris et al.²¹ reported that the concentration of H^+/OH^- ions at the O/W interface could alter droplet charge. The addition of GA to the water phase lowered the pH and weakened the charge of the emulsion droplets. Table S1 shows that the pH of the double emulsions decreased with increasing GA levels, with the GG group containing the highest GA levels and exhibiting the lowest pH. This reduction in pH likely weakened the electrostatic repulsive force between droplets, particularly in the GG group, leading to an increased CI and droplet size, indicating a decrease in emulsion stability.

Encapsulation efficiency

Fig. 3D shows the encapsulation efficiency of water-soluble (EE_w) in double emulsions at various storage times. Tartrazine, used as a marker for the elution of the W_1 phase, was measured in the W_2 phase at 0, 1, 2, and 4 weeks. In fresh double emulsions (fresh, 0 week), the EE_w of the double emulsion decreased with droplet size and apparent viscosity, consistent with the findings of Kwak et al.⁶. As storage time progressed, a corresponding decline in EE_w was observed. Notably, the PO emulsion showed a more significant decrease than the CO emulsion. Furthermore, NG and GG, in which GA was incorporated into the W_2 phase, exhibited a substantial reduction in EE_w .

The rate of emulsion separation depend on the droplet size and density difference between the inner and outer phases, and inversely on the viscosity of the emulsions, as described by

Stokes' law¹⁴. A decrease in viscosity reduces the resistance to the upward movement of oil droplets, whereas a slight increase in the density of the aqueous phase, due to dissolved GA, may enhance the density difference from the oil phase, accelerating phase separation. This dynamic likely had an adverse effect on EEW by reducing the spacing between droplets and increasing emulsion instability. Additionally, the reduced interdroplet spacing, coupled with the low ζ -potential of PO emulsions and the acidic conditions, likely diminished the repulsive forces between droplets²⁷, further decreasing the EEW . The localization of GA within the W_2 phase significantly influenced EEW , particularly in the NG and GG samples. The differences in EEW between the PO and CO emulsions warrant further investigation into the specific characteristics affecting these outcomes. Additionally, the observed correlation between decreasing viscosity and reduced EEW suggests that a systematic quantitative analysis is needed to better understand how viscosity affects the encapsulation efficiency.

Apparent viscosity

Fig. 4A–D shows that the apparent viscosity of all emulsions decreased with increasing shear rate, confirming that they were non-Newtonian pseudoplastic fluids. This behavior is primarily attributed to the disruption of droplet clusters and deformation of the emulsion network under shear, resulting in a structural breakdown¹². Typically, the viscosity of an emulsion increases with the higher volume fraction of the dispersed phase. In high internal phase emulsions, where the dispersed phase volume fraction exceeds 74%, droplets are closely packed, exhibiting semi-solid characteristics²⁸.

During storage, the viscosity of all emulsions decreased up to the 2-week storage period. Over time, phenomena such as flocculation, over-swelling of oil droplets, and expulsion of the W_1 droplet contributed to the increased thickness of the oil phase shell in the $W_1/O/W_2$ double emulsion, thereby reducing viscosity^{5,29}. Notably, the PO emulsion containing GA exhibits a

significant decrease in viscosity (Fig. 4 and Table S2). The lower viscosity of the PO emulsion is associated with faster emulsion separation than that of the CO emulsion, indicating reduced stability. In contrast, higher viscosity restricts the mobility and volumetric changes of the droplets, enhancing the overall emulsion stability⁵. The PO emulsion exhibited a higher CI than the CO emulsion (Fig. 3B). Interestingly, after four weeks of storage, an increase in viscosity was observed for all double emulsions (Fig. 4D). Since the viscosity measurements were taken from the surface region, this increase likely reflects an uneven distribution of emulsion droplets, as indicated by the CI results. Thus, the measured viscosity at the surface may represent a localized region with a higher concentration of droplets, rather than the bulk emulsion properties.

Thiobarbituric acid reactive substance (TBARS) assay

Fig. 5A shows the TBARS values of the double emulsions containing GA and PO over the storage period. Across all samples, TBARS values increased with storage time, with the NN group (without added GA) exhibiting the most significant increase. In an emulsion system, oxidation occurs predominantly at the interface between the two phases (air/oil and oil/water). Peroxides, which are surface-active, can migrate to the oil-water interface, where they can donate hydrogen atoms and are quenched²⁴. Polyphenolic compounds, such as GA, act as antioxidants by scavenging free radicals and donating hydrogen atoms to terminate the lipid oxidation chain reaction³⁰.

Although GA added to the W_1 phase may compete with the PGPR for adsorption at the W_1/O interface¹¹, the primary site of oxidation is the O/W_2 interface. However, the results of EE_w (Fig. 3D) indicate that the GA encapsulated in the W_1 phase was released into the W_2 phase during preparation and storage. Notably, even a small amount of GA released from the W_1 phase into the W_2 phase during storage may significantly contribute to oxidative protection

at the critical O/W interface. Furthermore, the double emulsion with GA directly in the W_2 phase exhibited lower TBARS values than those with GA in the W_1 phase or without any GA. According to Losada-Barreiro et al.²³, the distribution of hydrophilic antioxidants, such as GA, is influenced by the HLB of non-ionic surfactants, with more than 40% of the hydrophilic antioxidant typically localizing at the interfacial region, regardless of surfactant concentration and HLB. This localization enables the GA in the W_2 phase to effectively inhibit oxidation of the oil phase.

The lower antioxidant performance observed in the GG group, despite its higher GA content, can be attributed to the reduced dissociation of GA at lower pH levels. At lower pH values, a higher proportion of GA remains undissociated, which may reduce its interfacial localization and limit its effectiveness in inhibiting lipid oxidation. Mei et al.³¹ noted that at acidic pH conditions of approximately 3, low concentrations of galloyl derivatives (gallic acid, methyl gallate, and gallamide) may act as prooxidants. Specifically, at pH 3, increased protonation enhances the hydrophobicity and dispersion by non-ionic surfactants, potentially reducing the decreasing potential of GA relative to iron, leading to prooxidant behavior in the TBARS assay. Although the concentration of GA used in this experiment (approximately 30 mM) is considerably high and should favor antioxidant activity, Mei et al.³¹ also reported that undissociated GA could be sequestered by non-ionic surfactants, diminishing the total phenolic content available in the dispersion medium.

Given that the pKa of the carboxyl group in GA is 4.4³², the pH of the GG samples (2.94–3.34) is further from the pKa than that of the NG samples (3.24–3.54). This indicates that GA is less dissociated in the presence of GG, resulting in a higher proportion of its molecules being encapsulated by non-ionic surfactants. Consequently, despite the higher dosage of GA in the GG group, the NG group exhibited stronger antioxidant efficacy. This phenomenon may be attributed to the higher CI observed at lower pH, which promotes a more pronounced separation

between the W_1/O emulsion and W_2 phase. The reduced presence of the W_2 phase surrounding the oil droplets decreased the availability of GA at the interface, thereby contributing to higher TBARS values.

Total carotenoid content

The C^R , C^Y , and C^T values of the PO emulsions during storage are shown in Table 3. The PO double emulsions without the added antioxidant GA exhibited a lower C^T immediately after preparation than the emulsions containing GA. This may be due to the antioxidant effects of GA on heat-sensitive carotenoids. According to Gu et al.³³, the incorporation of catechins, a group of flavonoids, into emulsions containing beta-carotene enhances their thermal stability. The initial color measurements showed lower a^* and b^* values in the PO-NN group, which did not contain GA (Table 2). After 1 week of storage, the C^T exhibited a descending trend, with the GG group containing the highest levels, followed by the NG, GN, and NN groups, which had the lowest amount of added GA. After four weeks of storage, the C^T of the NN sample exhibited a notable decline. Among the other GA added groups, NG, GG, and GN showed the highest C^R values. These results are consistent with the TBARS findings for the PO emulsions, supporting the efficacy of adding GA to the external aqueous phase of the double emulsion to improve oxidative stability.

Antioxidant capacity

To comprehensively evaluate the antioxidant potential of W/O/W double emulsions, DPPH, ABTS, and FRAP assays were conducted over a four-week storage period under two different oil-phase conditions: canola oil alone and canola oil supplemented with 0.5% PO (Fig. 5B–D). Overall, emulsions containing GA (NG, GN, and GG) exhibited significantly higher

antioxidant activity than the control (NN), confirming the efficacy of GA in enhancing oxidative stability owing to its established radical scavenging and metal-chelating properties^{3,34}.

Among these formulations, the GG emulsion containing GA in both the inner (W_1) and outer (W_2) aqueous phases consistently demonstrated the highest radical-scavenging capacity (DPPH and ABTS) and FRAP, particularly in emulsions incorporating PO. This indicated improved antioxidant effect from the dual-phase distribution, enabling GA to intercept radicals at both the W_1/O and O/W_2 interfaces^{17,23}. Such localization can be strategically applied in the design of emulsion systems for encapsulating oxidation-sensitive bioactive molecules, thereby enhancing both protection and delivery efficiency.

The addition of PO further amplified the antioxidant activities across all assays. The carotenoids (capsanthin and capsorubin) present in PO significantly contributed to radical scavenging within the lipid domains, while stabilizing the interfacial membrane structure¹². Unlike previous studies that focused on single-phase antioxidants⁵, the combination of hydrophilic (GA) and lipophilic (PO) antioxidants at distinct interfaces generated a multilayered oxidative barrier, enhancing oxidative resistance while simultaneously altering the physical stability of the double emulsions consubstantially compared to single-antioxidant formulation.

W_2 is particularly critical due to its direct contact with the external environment, which makes it highly susceptible to oxidative agents such as dissolved oxygen and transition metals. Placing GA in W_2 effectively intercepts these reactive species before they reach the interface, thereby efficiently preventing the onset of oxidation. In contrast, antioxidants confined within W_1 show limited effectiveness in counteracting external oxidative stress owing to restricted accessibility. Hence, external aqueous phase localization of hydrophilic antioxidants has emerged as an effective strategy for enhancing the emulsion oxidative stability³⁴. DPPH, ABTS, and FRAP assays evaluate the anti-radical capacity of antioxidants under simplified conditions

and do not directly reflect the inhibition of lipid oxidation in complex food systems. Therefore, higher anti-radical values indicate the presence and potential availability of antioxidant compounds rather than definitive antioxidant efficiency. This interpretation aligns with the findings of Cravero et al.³⁵ reported that antioxidant administration is more effective when provided all at once rather than in progressive doses prior to the onset of lipid oxidation.

However, a slight inconsistency emerged in the TBARS results, where GG emulsions exhibited marginally lower inhibition than NG formulations, particularly under acidic conditions. This discrepancy highlights the complex nature of oxidative mechanisms, which are influenced by factors such as pH, interfacial composition, and emulsifier interactions. TBARS specifically quantifies malondialdehyde (MDA), a sensitive marker significantly influenced by environmental conditions, which may not fully reflect the broader antioxidant potential assessed using the DPPH, ABTS, and FRAP assays. Therefore, utilizing multiple complementary assays is crucial for accurately evaluating antioxidant efficacy in multiphase systems or lipid deterioration measurements, such as chemical, volatile or sensory indicators^{36,37}.

The observed low antioxidant activity of the GG sample is hypothesized to result from the combined effects of these two factors. One of these effects is attributed to GA-induced prooxidant activity, while the other is associated with stratification. Illustrated by Mei et al., under acidic conditions (approximately pH 3.0), a larger proportion of GA remains undissociated, enabling it to reduce ferric ions (Fe^{3+}) to ferrous ions (Fe^{2+})^{31,38}. The generated ferrous ions may subsequently react with lipid hydroperoxides formed during storage, generating reactive oxygen species that promote lipid oxidation. Therefore, under low pH conditions, GA may exhibit prooxidant behavior when its concentration is insufficient to scavenge the radicals produced. Furthermore, the high CI of the GG sample reduced the effective interfacial region in contact with both the W_1/O droplets and the outer aqueous phase³⁹. Since antioxidant action in emulsions mainly occurs at the oil–water interface, this loss of interfacial area

limited the amount of GA retained at the interface. The reduced interfacial presence of GA explains the lower oxidative stability observed in the GG formulation despite its higher total GA content. Although the concentration of transition metals was not directly quantified in this study, trace levels of iron and other metals are typically present in salts and raw materials used in food emulsions and could participate in GA-mediated $\text{Fe}^{3+}/\text{Fe}^{2+}$ redox cycling under acidic conditions. These findings suggest that antioxidant efficacy and physical stability of the $W_1/O/W_2$ double emulsions are critically dependent on the spatial localization of antioxidants across distinct phases. The GG formulation, which combines GA in both the W_1 and W_2 phases with PO in the oil phase, demonstrated superior antioxidant activity owing to the dual-layered protection at both interfaces and lipid domains. However, formulations such as NG (GA in W_2 only), despite having a slightly lower antioxidant performance, showed superior physical stability, including reduced creaming and stable viscosity.

Ultimately, strategically positioning antioxidants at specific interfacial regions enhances oxidative protection and improves structural integrity under prolonged storage. These insights offer valuable guidance for developing stable and robust double emulsions for practical applications in the food, nutraceutical, and cosmetic industries^{1,17}.

In conclusion, this study demonstrates that the incorporation and spatial localization of lipophilic paprika oleoresin and hydrophilic gallic acid distinctly affect the oxidative and structural stability of double emulsions. Although blank emulsions exhibited relatively stable droplet structures, the introduction of antioxidants altered their interfacial characteristics in a phase-dependent manner. GA in the outer aqueous phase enhanced antioxidant capacity but reduced ζ -potential and viscosity, while dual incorporation yielded the highest antioxidant activity with compromised physical stability. These findings suggest that antioxidant localization influences both oxidative protection and emulsion integrity, as interfacial adsorption dynamics and pH-related charge reduction may be involved in the observed stability

changes. In conclusion, this work provides a mechanistic basis for designing phase-oriented antioxidant strategies to achieve a balance between oxidative protection and physical stability in stable double emulsion systems applicable to high-viscosity food products such as sauces, dressings, and functional spreads.

Methods

Materials and reagents

Gallic acid (GA) was purchased from Sigma-Aldrich (St. Louis, MO, US). The PGPR (PT. MusimMas, Singapore) and Tween® 80 (Daejung, Seoul, Korea) were used as emulsifiers for the oil phase and outer aqueous phase, respectively. Canola oil (Sajo-Haepyo, Seoul, Korea) was purchased locally and used as the oil phase for the double emulsions. Paprika oleoresin (PO, Plant Lipids, Kerala, India) was added to canola oil at a concentration of 0.5% (w/w). Tartrazine (Sigma-Aldrich, St. Louis, US) was used as a marker of encapsulation efficiency. Trichloroacetic acid (Daejung), hydrochloric acid (HCl; Daejung), and thiobarbituric acid (TBA; Sigma-Aldrich) were used for lipid oxidation measurements. Sodium citrate (Samchun, Seoul, South Korea) and n-hexane (Daejung Chemicals, Siheung-si, South Korea) were used to determine total carotenoid content.

Preparation of double emulsions

The compositions of the double emulsions are listed in Table S3. The inner aqueous phase (W_1) consisted of distilled water containing 1.8% (w/w) KCl alone or 1.8% (w/w) KCl with 0.5% (w/w) GA. The blank control (NN) consisted of canola oil containing 5% (w/w) PGPR alone or 5% PGPR (blank control emulsion) with 0.5% (w/w) PO. For PO-containing samples, the oil phase consisted of canola oil with 5% (w/w) PGPR and 0.5% (w/w) PO. The outer aqueous phase (W_2) contained NaCl (1.4% w/w) and Tween® 80 (2% w/w), with or

without GA (0.5%). The following abbreviations are used for samples based on the localization of GA: double emulsion without gallic acid (NN), double emulsions containing gallic acid in W_1 phase (GN), double emulsions containing gallic acid in W_2 phase (NG), double emulsions containing gallic acid in W_1 and W_2 phase (GG). The GA content in the inner and outer aqueous phases was fixed at 0.5% (w/w) to be far from the saturation point of GA³⁹. KCl and NaCl were used to adjust the osmotic pressure between the inner and outer aqueous phases to prevent droplet shrinkage or rupture during storage¹. Each phase was stirred overnight at 25°C for complete dissolution.

The W/O/W double emulsions were prepared according to the method described by Lee et al.¹, with slight modifications. Briefly, primary W_1/O emulsions containing 20% W_1 phase and 80% oil phase were prepared by slowly adding W_1 to the continuous oil phase at 700 rpm for 3 min using a propeller stirrer (Chang Shin Scientific Co., Ltd., South Korea). The coarse primary emulsion was then homogenized at 15,000 rpm for 5 min using a high-speed homogenizer (T25 digital IKA®; Ultra-Turrax®, Germany). Subsequently, the primary emulsion was slowly added to the continuous W_2 phase while stirring at 700 rpm for 3 min, and the coarse double emulsions were homogenized at 10,000 rpm for 3 min in an ice-bath. Fresh double emulsions were transferred to 50 mL conical tubes and stored at 4°C until analysis.

Interfacial tension measurement

The interfacial tension between the aqueous and oil phases was measured using the Du Nouy ring method with a tensiometer (Sigma 703D, KSV, MA, USA)⁵. Briefly, the aqueous phase was placed in a glass vessel and the oil phase was gently placed onto it. The ring was immersed in the aqueous phase and slowly raised through the interface until the maximum force was measured, which represent the interfacial tension (mN/m).

Morphology and droplet size analysis

The morphology of the double emulsions was analyzed using an optical microscope (CX31, Olympus Optical Co., Ltd., Tokyo, Japan) equipped with a CCD camera (3.0M, Olympus Optical Co., Ltd.) at 1,000× magnification. The mean droplet size was determined from microscopic images using ImageJ software, measuring at least 1,000 droplets per sample. Confocal laser scanning microscopy (CLSM; LSM 800; Carl Zeiss, Jena, Germany) was used to visualize the internal aqueous phase distribution within the emulsions. The oil phases were dyed with 0.01 wt% Nile Red in canola oil. CLSM images were captured using 488 nm excitation and a 64× oil immersion objective.

Color measurement

Color measurements were conducted using a chroma meter (CR-200, Konica Minolta, Tokyo, Japan), calibrated with a standard white plate ($L^* = 97.83$, $a^* = -0.43$, $b^* = 1.98$). Samples were placed in 5 mm Petri dishes (50 mm diameter, 5 mm thickness). Color values were reported in the Commission International de l'Eclairage value (L^* , whiteness or brightness; a^* redness; b^* , yellowness) with illuminant D65 and a 2 mm target.

The whiteness value was calculated as reported by Zhou et al.⁸, Eq. (1):

$$\text{Whiteness value} = 100 - \sqrt{(100 - L^*)^2 + a^{*2} + b^{*2}} \quad (1)$$

Appearance and creaming index

The W/O/W double emulsions (15 mm diameter × 65 mm height glass vials) were stored for 4 weeks at 4°C. The creaming index (CI) was determined by visually observing the height of the serum layer, which was photographed using a digital camera (Sony a350, Tokyo, Japan). CI was calculated using Eq. (2):

$$CI (\%) = \left(\frac{H_s}{H_T} \right) \times 100 \quad (2)$$

where H_s is the height of the serum layer (mm), and H_T is the total height of the emulsion sample (mm). In this study, H_T was fixed at 60 mm.

ζ-potential measurement

The ζ-potential of the W/O/W double emulsions was measured using a ζ-potential analyzer (Litesizer DLS 100, Anton Paar, Austria) at 25°C. The samples were diluted 1:2,000 (v/v) with distilled water before measurement.

pH measurement

The pH of the double emulsions and their phases were measured at room temperature (25°C) using a calibrated pH meter (Orion Benchtop 3-STAR; Thermo Fisher Scientific, CA, USA). Samples (5 mL) were placed in 15 mL conical tubes, and the electrode was immersed directly into the samples. Calibration was performed using standard solutions with pH values of 4, 7, and 10 (Thermo Fisher Scientific).

Encapsulation efficiency

The encapsulation efficiency (EE_w) of the W_1 phase was determined at 0, 1, and 2 weeks following the method described by Silva et al.², with slight modifications. Tartrazine was used as a marker to evaluate EE_w . Briefly, the control solutions were prepared by mixing the W_1 phase (0.6 mg/mL tartrazine) with the W_2 phase. The absorbance was measured at 435 nm, and the tartrazine concentration was calculated from a standard curve ($R^2=0.9989-0.9997$).

A W/O/W double emulsion containing tartrazine in the W_1 phase was prepared following the procedure outlined in Section 2.2. Immediately after preparation, 30 g of each emulsion

was placed into 50 mL conical tubes and centrifuged at 10,000 rpm for 30 min at 4°C (centrifuge-1736R, LaboGene, Daejeon, Korea). The aqueous phase was filtered through a 0.45 µm syringe filter, and the absorbance was measured at 435 nm using a UV/VIS spectrophotometer (Multiskan Go, Thermo Fisher Scientific). Blank samples were prepared without the markers. EEw was calculated according to Eq. (3):

$$EEw (\%) = 100 - \left(\frac{C_{mc}}{C_{mi}} \times 100 \right) \quad (3)$$

where C_{mc} is the marker concentration in the W_2 phase after centrifugation, and C_{mi} is the initial marker concentration added to the double emulsion.

Apparent viscosity

The apparent viscosity of the W/O/W emulsions was measured using a Rheometer® (MCR 302, Anton Paar, Graz, Austria) equipped with a parallel-plate geometry (PP25; plate diameter = 24.978 mm, torsional compliance = 0.001375 rad/Nm, gap = 1 mm). Measurements were performed over shear rates ranging from 0.1 to 100 s⁻¹ at 25°C.

Lipid oxidation

Lipid oxidation in the double emulsions was evaluated at TBARS assay. Briefly, 1 mL of emulsion was mixed with 2 mL of TBA reagent (5% trichloroacetic acid and 0.375% thiobarbituric acid dissolved in 0.25 M HCl). The mixture was heated at 95°C for 15 min, cooled to 25°C, and centrifuged at 1,000 rpm for 15 min. Absorbance was measured at 532 nm and TBARS concentrations were calculated from a standard curve using 1,1,3,3-tetramethoxypropane (malondialdehyde equivalent, R²=0.9997).

Total carotenoid content

Total carotenoid content of the double emulsions was measured according to the methodology described by Hornero-Méndez and Mínguez-Mosquera⁴⁰. Briefly, 0.95 g of the double emulsions was diluted in 10 mL of a 10% (w/v) sodium citrate solution and sonicated for 20 min. Subsequently, 20 mL of hexane was added and the mixture was centrifuged at 8,000 rpm for 15 min. Absorbance was recorded at 472 and 508 nm. The isochromatic red and the yellow fractions, as well as the total carotenoid content, were calculated using Eq. (4), (5), (6):

$$C^R = \frac{A_{508} \times 2144.0 - A_{472} \times 403.3}{270.9} \quad (4)$$

$$C^Y = \frac{A_{472} \times 1724.3 - A_{508} \times 2450.1}{270.9} \quad (5)$$

$$C^T = C^R + C^Y \quad (6)$$

where C^R represents the content of the isochromatic red fraction, C^Y represents the yellow isochromatic fraction, C^T represents the total carotenoid content, and A_{472} and A_{508} represent the absorbance values at 472 and 508 nm, respectively.

Determination of Antioxidant Capacity

The double emulsions were stored in a refrigerator at 4°C for 4 weeks, and their antioxidant activity was evaluated at weeks 0, 1, 2, and 4 using the 2,2-diphenyl-1-picrylhydrazyl (DPPH), 2,2'-azino-bis(3-ethylbenzothiazoline-6-sulfonic acid) (ABTS), and ferric reducing antioxidant power (FRAP) assays⁴¹.

For the DPPH assay, 0.1 mL of the sample was mixed with 0.1 mL of 0.2 mM DPPH solution (Sigma-Aldrich, St. Louis, MO, USA) and incubated in the dark for 30 min at 25°C. The absorbance was measured at 517 nm using a spectrophotometer (Multiskan GO, Thermo

Scientific, Waltham, MA, USA). Methanol (0.1 mL) was used as the control. To correct the intrinsic color of the sample, an additional blank was prepared by replacing the DPPH solution with methanol, and absorbance was measured using the same procedure.

For the ABTS assay, the ABTS radical cation was generated by reacting a 7.0 mM ABTS aqueous solution with a 2.45 mM potassium persulfate ($K_2S_2O_8$) solution in equal volumes, followed by incubation in the dark for 12 h. The resulting ABTS solution was diluted with ultrapure water and mixed with the sample or buffer. After incubation in the dark for 6 min, absorbance was measured at 729 nm using a UV spectrophotometer (UV-1601, Shimadzu, Kyoto, Japan).

For the FRAP assay, the working reagent was freshly prepared by mixing 10 volumes of 300 mM acetate buffer (pH 3.6), one volume of 10 mM 2,4,6-tri(2-pyridyl)-s-triazine (TPTZ) in 40 mM hydrochloric acid, and one volume of 20 mM ferric chloride ($FeCl_3$). A 100 μ L aliquot of the sample and 300 μ L of deionized water were added to 3 mL of the freshly prepared FRAP reagent. The mixture was incubated in a water bath at 37°C for 30 min, and the absorbance was measured at 593 nm using a spectrophotometer (Multiskan GO, Thermo Scientific, Waltham, MA, USA). A sample blank was prepared using an acetate buffer instead of the sample. The FRAP value was calculated based on the difference in absorbance between the sample and the blank, and a standard curve was constructed using various ferrous sulfate heptahydrate ($FeSO_4 \cdot 7H_2O$) concentrations. Results were expressed as mmol Fe^{2+} /g of sample. All measurements were performed in triplicate.

Statistical analysis

All experimental results were expressed as mean \pm standard deviation of at least three independent experiments. Statistical analyses were conducted using SPSS software (version 27.0; SPSS Inc., Chicago, IL, USA). Differences among mean values were evaluated using

one-way analysis of variance (ANOVA) followed by Duncan's multiple range test, with statistical significance defined at $p < 0.05$.

Data availability

The datasets generated and/or analyzed during the current study are available from the corresponding author on reasonable request.

Acknowledgment

This work was supported under the framework of the International Cooperation Program managed by the National Research Foundation of Korea (Grant No. RS-2023-NR121115). This paper was supported by the KU Research Professor Program of Konkuk University.

Author contributions

S.J.: Investigation, Data curation, Formal analysis, Methodology, Writing - Original Draft; J.J.: Investigation, Methodology, Data curation; G.S.: Validation, Methodology; S.S.: Methodology, Validation; M.J.C.: Conceptualization, Supervision, project administration, Writing - Original Draft, Writing - Review & Editing, J.L.: Methodology, Software, Writing - Original Draft, Writing - Review & Editing.

Competing interests

The authors declare no competing interests.

References

1. Lee, J. et al. Influence of different electrolytes and oils on the stability of W₁/O/W₂ double emulsion during storage and in vitro digestion. *Food Sci. Biotechnol.* **32**(11), 1515–1529 (2023). <https://doi.org/10.1007/s10068-023-01282-5>
2. Silva, W. et al. Double emulsions as potential fat replacers with gallic acid and quercetin nanoemulsions in the whgaqueous phases. *Food Chem.* **253**, 71–78 (2018). <https://doi.org/10.1016/j.foodchem.2018.01.128>
3. Heidari, F. et al. Stability and release mechanisms of double emulsions loaded with bioactive compounds: A critical review. *Adv. Colloid Interface Sci.* **299**, 102567 (2022). <https://doi.org/10.1016/j.cis.2021.102567>
4. Brewer, M. S. Natural antioxidants: sources, compounds, mechanisms of action, and potential applications. *Compr. Rev. Food Sci. Food Saf.* **10**(4), 221–247 (2011). <https://doi.org/10.1111/j.1541-4337.2011.00156.x>
5. Hwang, W., Lee, J., & Choi, M. J. Optimization and characterization of high internal phase double emulsion (HIPDE) stabilized by with soybean protein isolate, gallic acid and xanthan gum. *Int. J. Biol. Macromol.* **264**, 130562 (2024). <https://doi.org/10.1016/j.ijbiomac.2024.130562>
6. Kwak, E. et al. Effect of electrolytes in the water phase on the stability of W₁/O/W₂ double emulsions. *Colloids Surf. A: Physicochem. Eng. Asp.* **650**, 129471 (2022). <https://doi.org/10.1016/j.colsurfa.2022.129471>
7. Ghelichi, S. et al. Oxidation and oxidative stability in emulsions. *Compr. Rev. Food Sci. Food Saf.* **22**(3), 1864–1901 (2023). <https://doi.org/10.1111/1541-4337.13134>
8. Bilawal, A. et al. Engineering stable gels: Whey protein isolate microgel-induced complexation with β-cyclodextrin in high internal phase emulsion gel. *Food Hydrocoll.* **168**, 111559 (2025). <https://doi.org/10.1016/j.foodhyd.2025.111559>
9. Bilawal, A. et al. Synergistic effects of ultrasound, pH-shifting and transglutaminase on high internal phase Pickering emulsion stabilized by whey protein isolate microgel particles. *Int. J. Biol. Macromol.* **322**(2), 146735 (2025). <https://doi.org/10.1016/j.ijbiomac.2025.146735>
10. Delmondes, P. H., & Stefani, R. Computational study of natural phenolic acid solubility and their interactions with chitosan. *MOL2NET* (2016). <https://sciforum.net/conference/mol2net-02>
11. Chevalier, R. C., Gomes, A., & Cunha, R. L. Tailoring W/O emulsions for application as inner phase of W/O/W emulsions: Modulation of the aqueous phase composition. *J. Food Eng.* **297**, 110482, (2021). <https://doi.org/10.1016/j.jfoodeng.2021.110482>
12. Li, C. et al. Oil-water interfacial dual-phase synergistic adsorption of capsanthin-cyanophycin in gelatin based high internal phase emulsions for multi-nozzle 3D printing. *Food Hydrocoll.* **158**, 110493 (2025). <https://doi.org/10.1016/j.foodhyd.2024.110493>
13. Rao, J., & McClements, D. J. Impact of lemon oil composition on formation and stability of model food and beverage emulsions. *Food Chem.* **134**, 749–757 (2012). <https://doi.org/10.1016/j.foodchem.2012.02.174>
14. Niu, H. et al. Multiscale combined techniques for evaluating emulsion stability: A critical review. *Adv. Colloid Interface Sci.* **311**, 102813 (2023). <https://doi.org/10.1016/j.cis.2022.102813>
15. Salvia-Trujillo, L. et al. Physicochemical characterization and antimicrobial activity of food-grade emulsions and nanoemulsions incorporating essential oils. *Food Hydrocoll.* **43**, 547–556 (2015). <https://doi.org/10.1016/j.foodhyd.2014.07.012>

16. Chantrapornchai, W., Clydesdale, F., & McClements, D. J. Influence of droplet characteristics on the optical properties of colored oil-in-water emulsions. *Colloids Surf. A: Physicochem. Eng. Asp.* **155**(2–3), 373–382 (1999). [https://doi.org/10.1016/S0927-7757\(99\)00004-7](https://doi.org/10.1016/S0927-7757(99)00004-7)
17. Wu, M. H. et al. Effects of emulsifier type and environmental stress on the stability of curcumin emulsion. *J. Dispers. Sci. Technol.* **38**(10), 1375–1380 (2017). <https://doi.org/10.1080/01932691.2016.1227713>
18. Doost, A. S. et al. Influence of non-ionic emulsifier type on the stability of cinnamaldehyde nanoemulsions: A comparison of polysorbate 80 and hydrophobically modified inulin. *Food Chem.* **258**, 237–244 (2018). <https://doi.org/10.1016/j.foodchem.2018.03.078>
19. Saari, N. H. M., & Chua, L. S. Nano-based products in beverage industry. In *Nanoengineering in the beverage industry* (pp. 405–436). Academic Press (2020), <https://doi.org/10.1016/B978-0-12-816677-2.00014-4>
20. de Aguiar, A. C. et al. Encapsulation of pepper oleoresin by supercritical fluid extraction of emulsions. *J. Supercrit. Fluids* **112**, 37–43 (2016). <https://doi.org/10.1016/j.supflu.2016.02.009>
21. de Moraes, J. M. et al. Characterization and evaluation of electrolyte influence on canola oil/water nano-emulsion, *J. Dispers. Sci. Technol.* **27**(7), 1009–1014, (2006). <https://doi.org/10.1080/01932690600767056>
22. Sharif, H. R. et al. Physicochemical stability of β -carotene and α -tocopherol enriched nanoemulsions: Influence of carrier oil, emulsifier and antioxidant. *Colloids Surf. A: Physicochem. Eng. Asp.* **529**, 550–559 (2017). <https://doi.org/10.1016/j.colsurfa.2017.05.076>
23. Losada-Barreiro, S., Sánchez-Paz, V., & Bravo-Díaz, C. Effects of emulsifier hydrophile–lipophile balance and emulsifier concentration on the distributions of gallic acid, propyl gallate, and α -tocopherol in corn oil emulsions. *J. Colloid Interface Sci.* **389**(1), 1–9 (2013). <https://doi.org/10.1016/j.jcis.2012.07.036>
24. Zhao, Z. et al. Interfacial engineering of Pickering emulsion co-stabilized by zein nanoparticles and tween 20: Effects of the particle size on the interfacial concentration of gallic acid and the oxidative stability. *Nanomaterials* **10**(6), 1068 (2020). <https://doi.org/10.3390/nano10061068>
25. Flores-Andrade, E. et al. Carotenoid nanoemulsions stabilized by natural emulsifiers: Whey protein, gum Arabic, and soy lecithin. *J. Food Eng.* **290**, 110208 (2021). <https://doi.org/10.1016/j.jfoodeng.2020.110208>
26. Di Mattia, C. D. et al. Effect of phenolic antioxidants on the dispersion state and chemical stability of olive oil O/W emulsions. *Food Res. Int.* **42**(8), 1163–1170 (2009). <https://doi.org/10.1016/j.foodres.2009.05.017>
27. Hong, I. K. Kim, S. I., & Lee, S. B. Effects of HLB value on oil-in-water emulsions: Droplet size, rheological behavior, zeta-potential, and creaming index. *J. Ing. Eng. Chem.* **67**, 123–131 (2018). <https://doi.org/10.1016/j.jiec.2018.06.022>
28. Gao, H. et al. Review of recent advances in the preparation, properties, and applications of high internal phase emulsions. *Trends Food Sci. Technol.* **112**, 36–49 (2021). <https://doi.org/10.1016/j.tifs.2021.03.041>
29. Pal, R. Rheology of double emulsions. *J. Colloid Interface Sci.* **307**(2), 509–515 (2007). <https://doi.org/10.1016/j.jcis.2006.12.024>
30. Iqbal, S. et al. Impact of various parameters over the stability of water-in-vegetable oil emulsion. *Dispers. Sci. Technol.* **34**(11), 1618 (2012). <https://doi.org/10.1080/01932691.2012.743307>

31. Mei, L., McClements, D. J., & Decker, E. A. Lipid oxidation in emulsions as affected by charge status of antioxidants and emulsion droplets. *J. Agric. Food Chem.* **47**(6), 2267–2273 (1999). <https://doi.org/10.1021/jf980955p>
32. Huguenin, J., Ould Saad Hamady, S., & Bourson, P. Monitoring deprotonation of gallic acid by Raman spectroscopy. *J. Raman Spectrosc.* **46**(11), 1062–1066 (2015). <https://doi.org/10.1002/jrs.4752>
33. Gu, L. Protection of β -carotene from chemical degradation in emulsion-based delivery systems using antioxidant interfacial complexes: Catechin-egg white protein conjugates, *Food Res. Int.* **96**, 84–93 (2017). <https://doi.org/10.1016/j.foodres.2017.03.015>
34. Farooq, S. A comprehensive review on polarity, partitioning, and interactions of phenolic antioxidants at oil–water interface of food emulsions. *Compr. Rec. Food Sci. Food Saf.* **20**(5), 4250–4277 (2021). <https://doi.org/10.1111/1541-4337.12792>
35. Cravero, C. F., Juncos, N. S., Grosso, N. R., & Olmedo, R. H. (2024). Autoxidation interference assay to evaluate the protection against lipid oxidation of antioxidant administration: Comparison of the efficiency of progressive release or total administration. *Food Chemistry*, 444, 138580. <https://doi.org/10.1016/j.foodchem.2024.138580>
36. Huang, D., Ou, B., & Prior, R. L. The chemistry behind antioxidant capacity assays. *J. Agric. Food Chem.* **53**(6), 1841–1856 (2005). <https://doi.org/10.1021/jf030723c>
37. Zhong, Y., & Shahidi, F. Methods for the assessment of antioxidant activity in foods. In *Handbook of antioxidants for food preservation*. Woodhead Publishing 287–333 (2015). <https://doi.org/10.1016/B978-1-78242-089-7.00012-9>
38. Gomes, A., Costa, A. L. R., de Assis Perrechil, F., & da Cunha, R. L. (2016). Role of the phases composition on the incorporation of gallic acid in O/W and W/O emulsions. *Journal of Food Engineering*, 168, 205–214. <https://doi.org/10.1016/j.jfoodeng.2015.07.041>
39. Berton-Carabin, C. C., Ropers, M. H., & Genot, C. (2014). Lipid oxidation in oil-in-water emulsions: Involvement of the interfacial layer. *Compr. Rev. Food Sci. Food Saf.* **13**(5), 945–977. <https://doi.org/10.1111/1541-4337.12097>
40. Hornero-Méndez, D., & Mínguez-Mosquera, M. I. Rapid spectrophotometric determination of red and yellow isochromic carotenoid fractions in paprika and red pepper oleoresins. *J. Agric. Food Chem.* **49**(8), 3584–3588 (2001). <https://doi.org/10.1021/jf0104001>
41. Jo, Y.J., Cho, H. S. & Chun, J. Y. Antioxidant activity of β -cyclodextrin inclusion complexes containing trans-cinnamaldehyde by DPPH, ABTS and FRAP. *Food Sci. Biotechnol.* **30**, 807–814 (2021). <https://doi.org/10.1007/s10068-021-00914-y>

Fig. 1 Optical (A) and confocal laser scanning microscopic images (B) of fresh double emulsions with different compositions. NN, double emulsion without gallic acid; GN, double emulsions containing gallic acid in W_1 phase; NG, double emulsions containing gallic acid in W_2 phase; GG, double emulsions containing gallic acid in W_1 and W_2 phase.

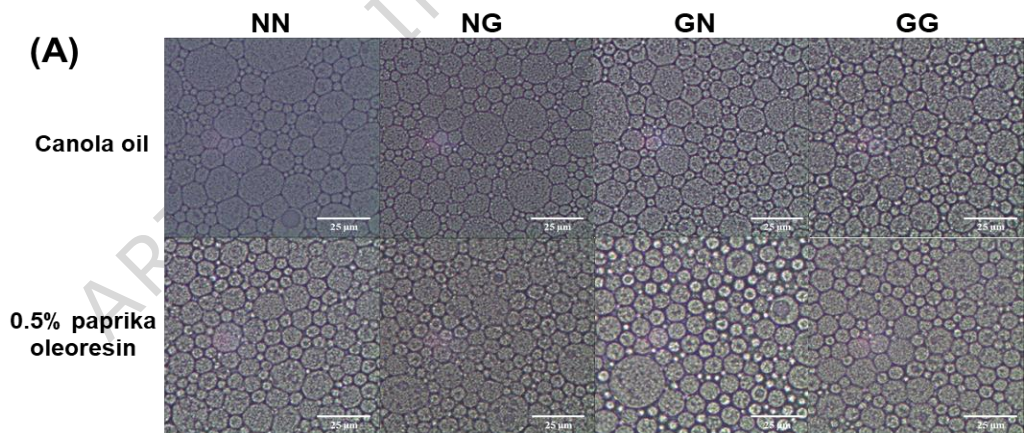
Fig. 2 Particle size (A) and whiteness value (B) of double emulsions with different storage periods and compositions. NN, double emulsion without gallic acid; GN, double emulsions containing gallic acid in W_1 phase; NG, double emulsions containing gallic acid in W_2 phase; GG, double emulsions containing gallic acid in W_1 and W_2 phase. Different lowercase letters within the same column and uppercase letters within the same row indicate significant differences ($p < 0.05$) according to Duncan's multiple range test following a one-way ANOVA.

Fig. 3 Appearance (A), creaming index (B), ζ -potential (C), and encapsulation efficiency of W_1 (EEw ; D) of double emulsions with different storage periods and compositions. NN, double emulsion without gallic acid; GN, double emulsions containing gallic acid in W_1 phase; NG, double emulsions containing gallic acid in W_2 phase; GG, double emulsions containing gallic acid in W_1 and W_2 phase. Different lowercase letters within the same column and uppercase letters within the same row indicate significant differences ($p < 0.05$) according to Duncan's multiple range test following a one-way ANOVA.

Fig. 4 Viscosity of double emulsions after fresh (A), 1 week (B), 2 weeks (C), and 4 weeks (D) with different compositions and storage periods. Black, double emulsions with canola oil in oil phase; Gray, double emulsions with 0.5% paprika oleoresin in oil phase; NN, double emulsion without gallic acid; GN, double emulsions containing gallic acid in W_1 phase; NG, double emulsions containing gallic acid in W_2 phase; GG, double emulsions containing gallic acid in W_1 and W_2 phase.

Fig. 5 The TBARS (A), DPPH (B), ABTS (C), and FRAP (D) assays of double emulsions with different storage periods and compositions. TBARS, thiobarbituric acid reactive substances; MDA, malondialdehyde equivalent; NN, double emulsion without gallic acid; GN, double emulsions containing gallic acid in W_1 phase; NG, double emulsions containing gallic acid in W_2 phase; GG, double emulsions containing gallic acid in W_1 and W_2 phase. Different lowercase letters within the same column and uppercase letters within the same row indicate significant differences ($p < 0.05$) according to Duncan's multiple range test following a one-way ANOVA.

Fig. 1



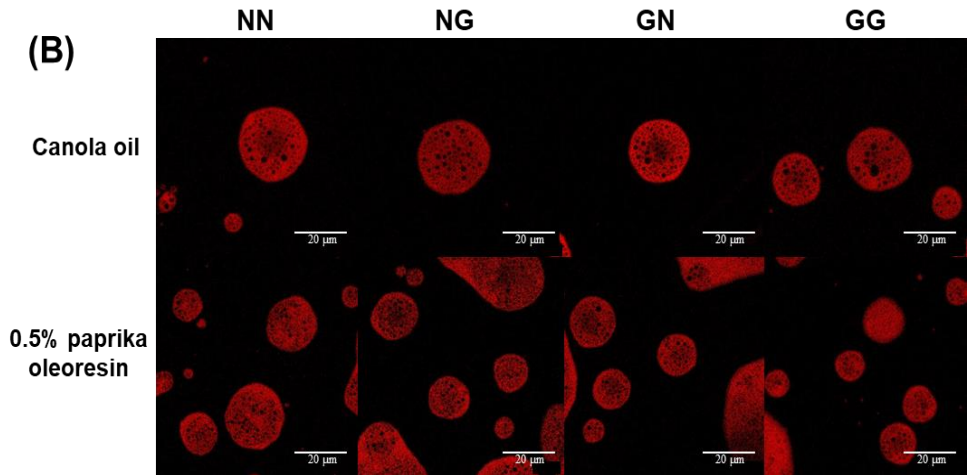
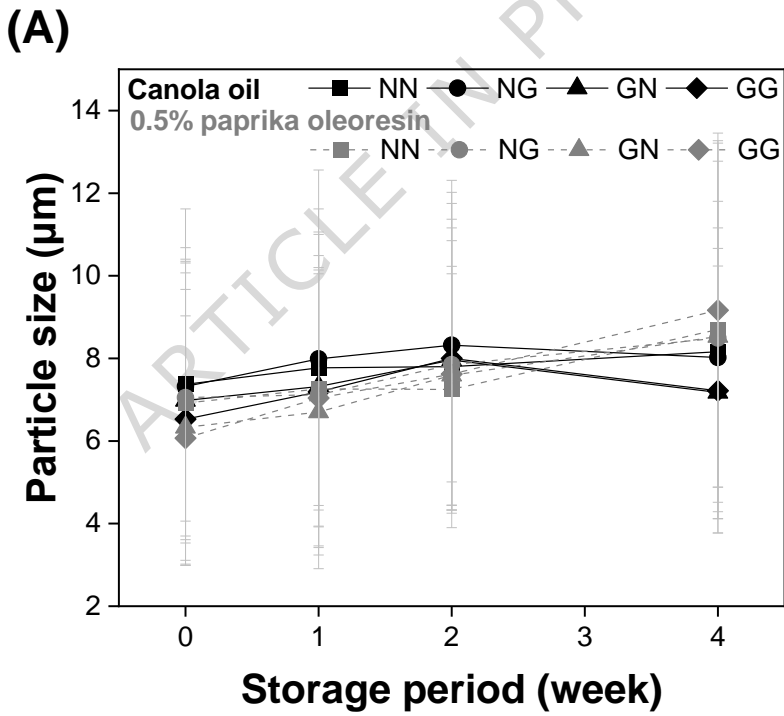


Fig. 2



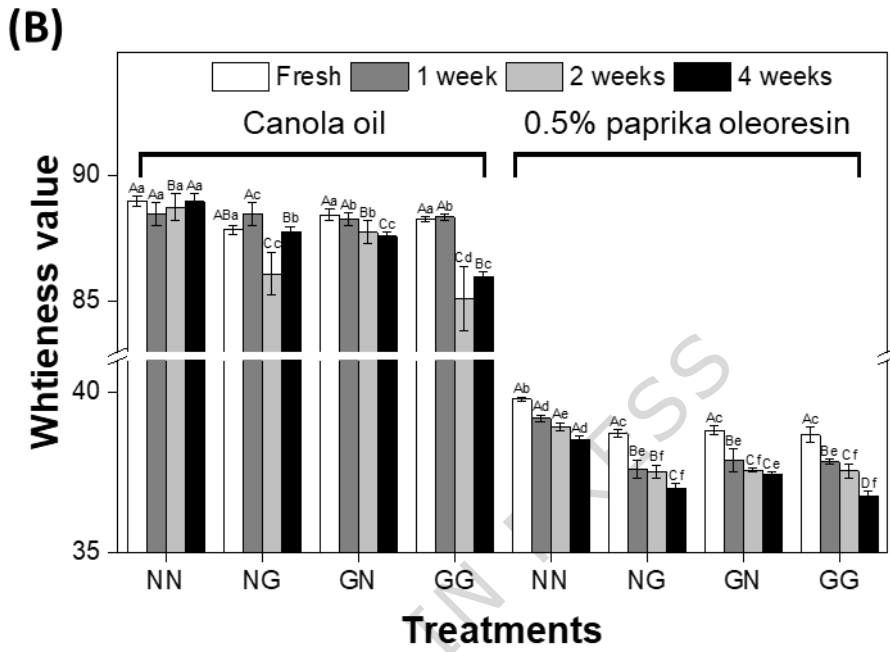
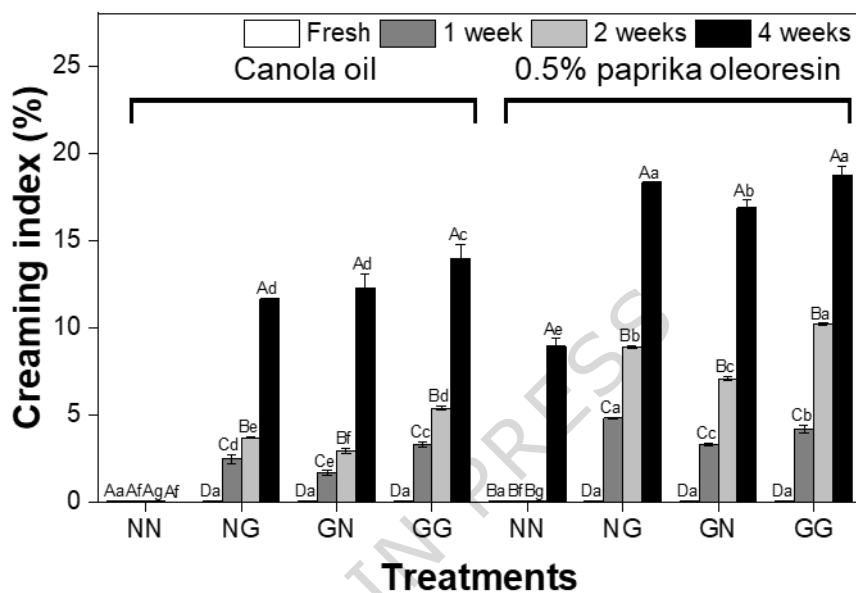
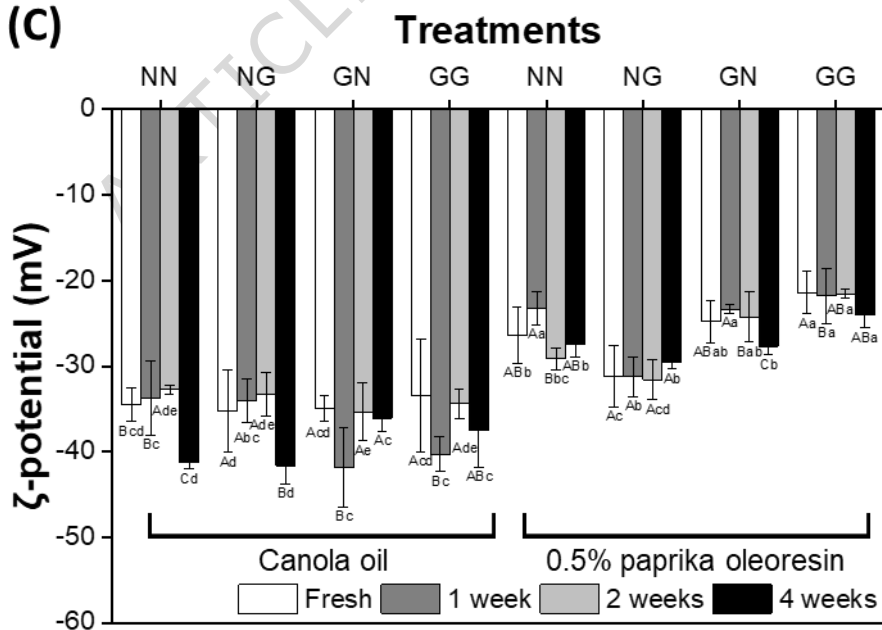


Fig. 3



(B)**(C)**

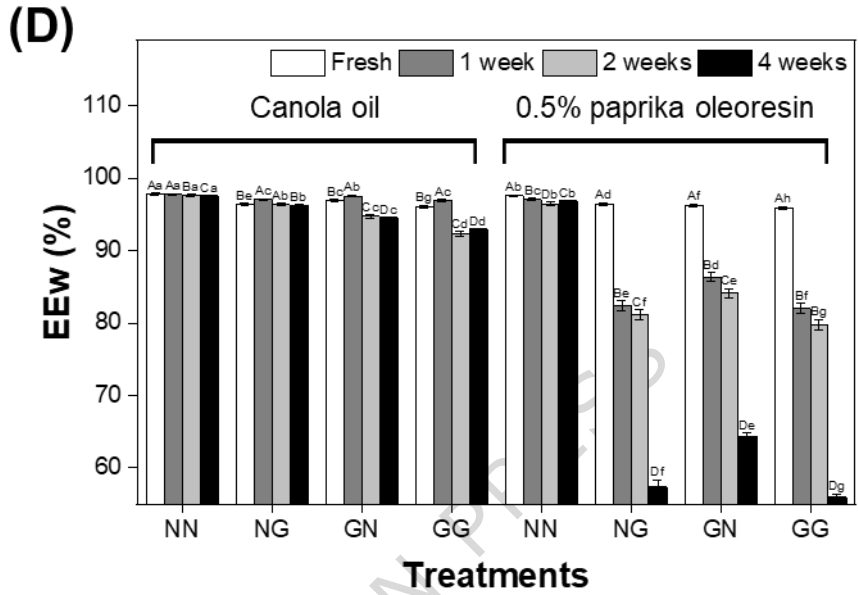
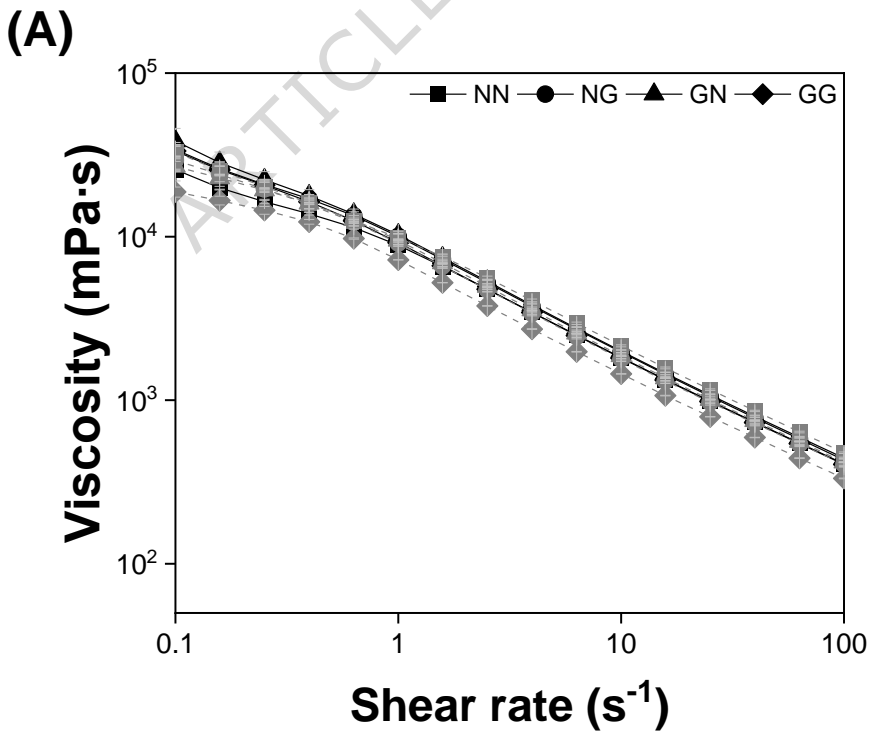
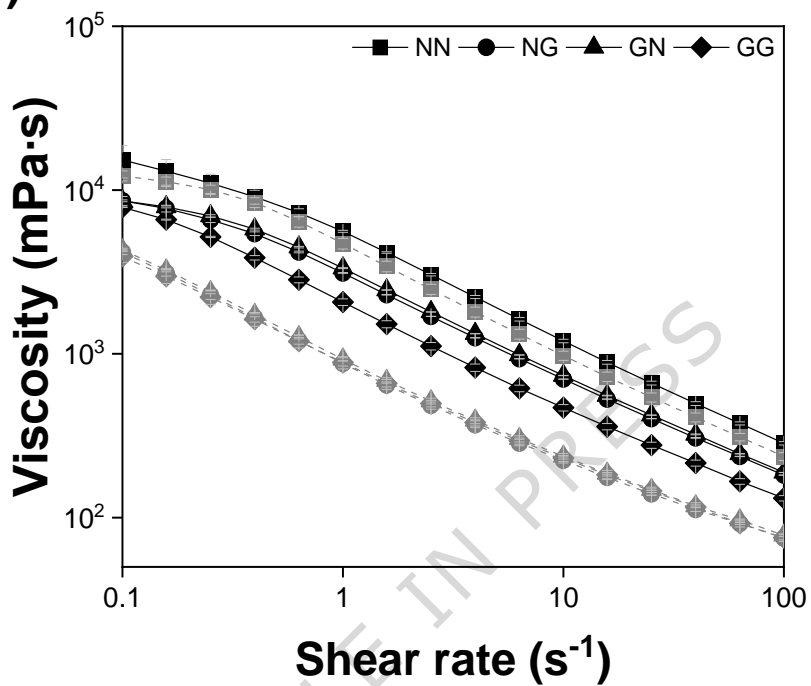


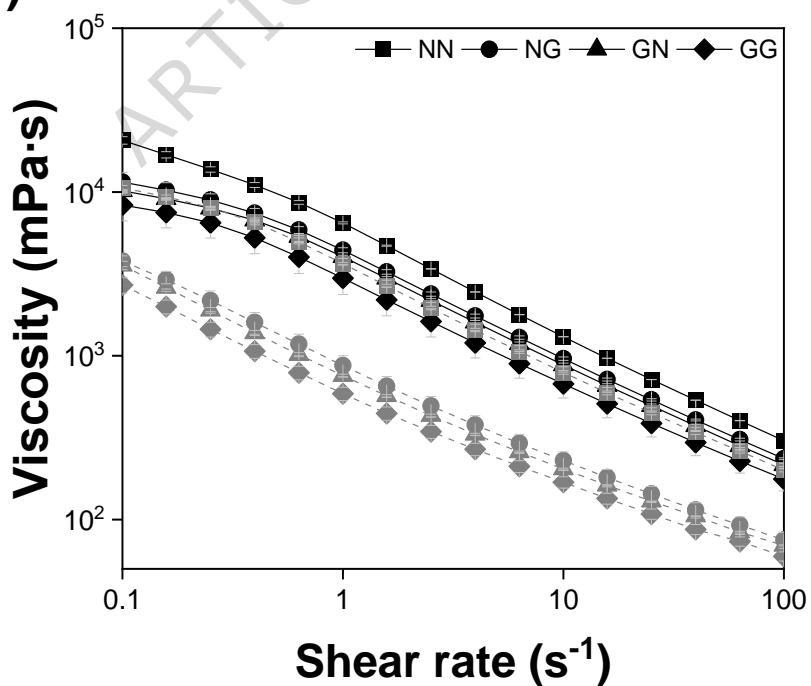
Fig. 4



(B)



(C)



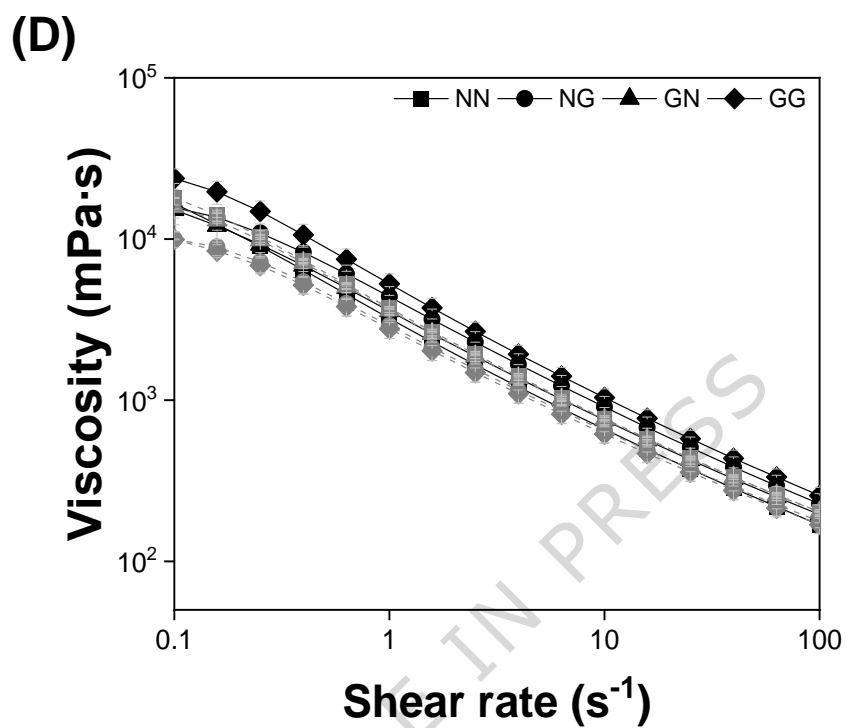
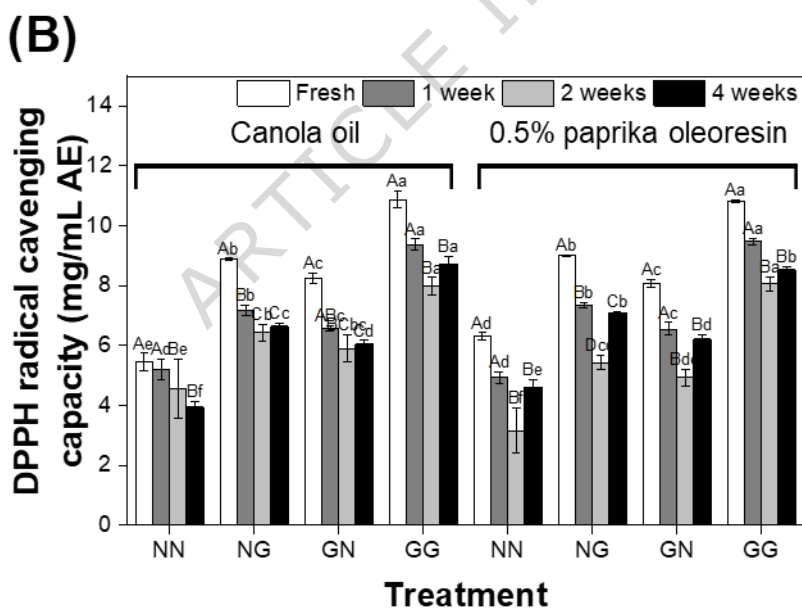
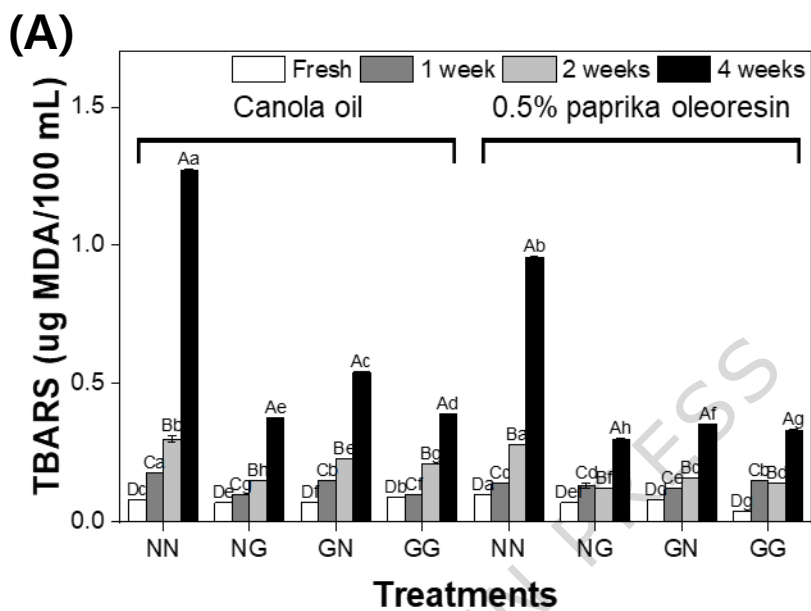
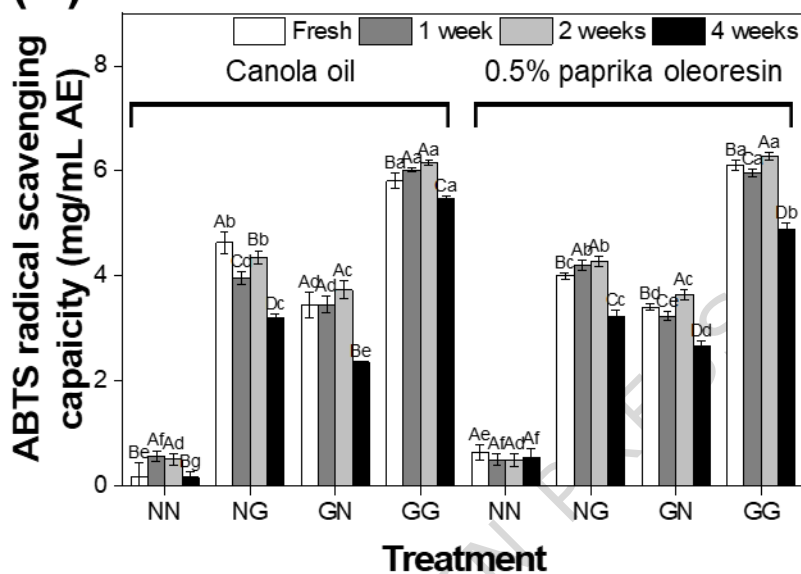


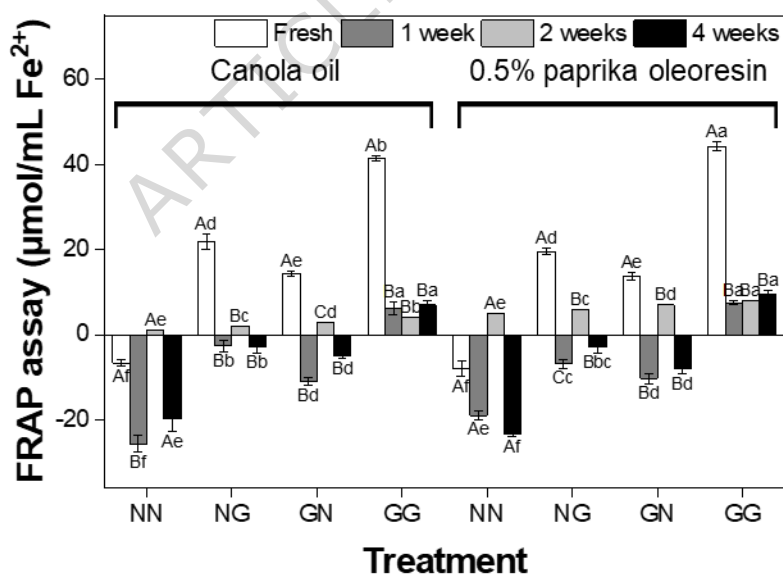
Fig. 5

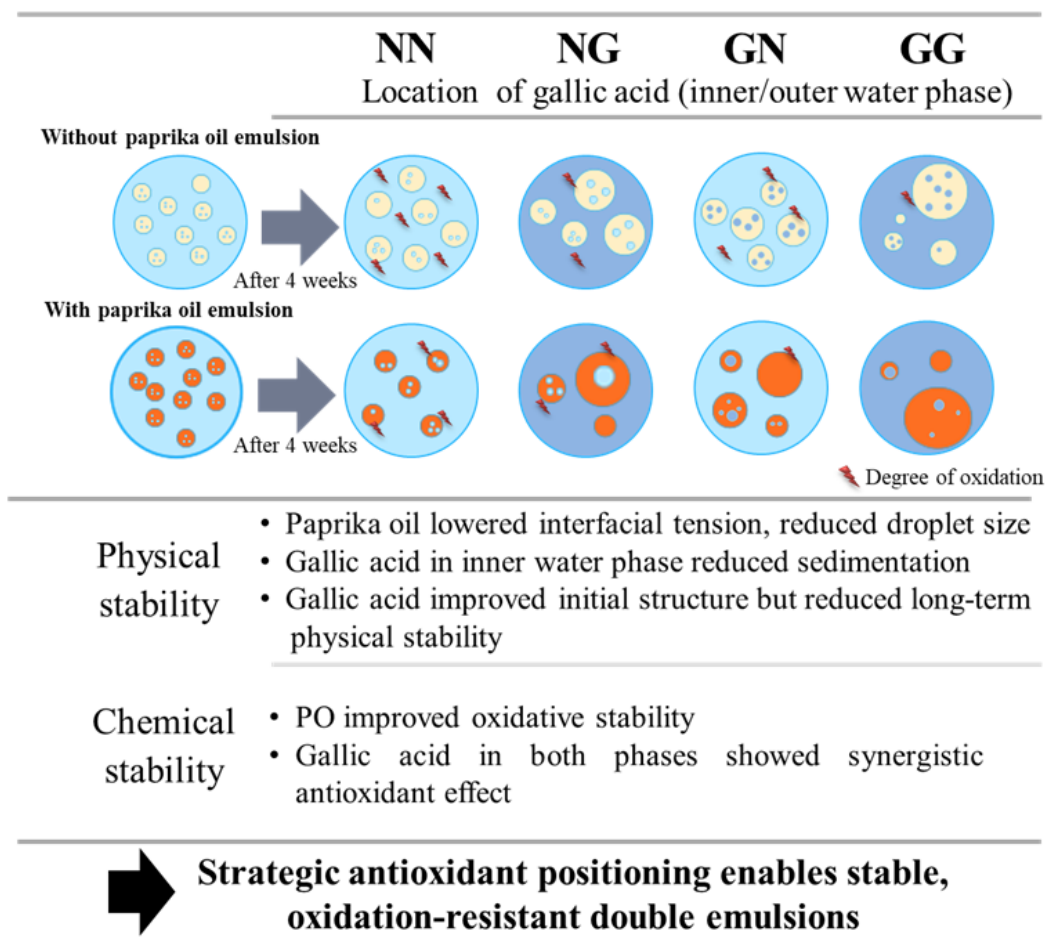


(C)



(D)



**Table 1 Interfacial tension between aqueous and oil phase of double emulsion**

	Gallic acid content (%)	Interfacial tension (mN/m)	
		Canola oil	0.5% paprika oleoresin in oil phase
W ₁	0.0	2.84±0.02 ^a	2.64±0.03 ^b
	0.5	2.62±0.06 ^b	2.52±0.09 ^c
W ₂	0.0	1.02±0.07 ^a	0.88±0.13 ^a
	0.5	1.00±0.01 ^a	0.71±0.08 ^b

W₁, 1.8% (w/w) KCl solution; W₂, 1.4% (w/w) NaCl solution with 2% Tween[®] 80 (w/w); The small letters in lower case mean the statistical significance within the same aqueous phase.

Table 2 CIE color value of double emulsions with different compositions

Treatment	Canola oil				0.5% paprika oleoresin in oil phase			
	Storage time (weeks)							
	0	1	2	4	0	1	2	4
<i>L*</i>								
NN	89.34±0.20 ^{ABa}	88.79±0.48 ^{BaA}	89.09±0.52 ^{ABa}	89.39±0.33 ^{AaA}	71.88±0.22 ^{BeA}	71.44±0.16 ^{CbA}	72.39±0.05 ^{AcA}	72.27±0.14 ^{AcA}
NG	88.27±0.21 ^{BcA}	89.03±0.45 ^{AaA}	86.53±0.81 ^{BcA}	88.29±0.22 ^{BbA}	72.12±0.12 ^{AdA}	71.53±0.17 ^{CbA}	71.80±0.06 ^{Bef}	71.65±0.16 ^{BCd}
GN	88.93±0.22 ^{AbA}	88.89±0.24 ^{AaA}	88.20±0.47 ^{BbA}	89.24±0.26 ^{AaA}	71.43±0.04 ^{BCf}	71.62±0.30 ^{Abb}	71.74±0.14 ^{Aef}	71.22±0.08 ^{CeA}
GG	88.81±0.10 ^{AbA}	88.95±0.10 ^{AaA}	85.55±1.29 ^{BdA}	88.17±0.15 ^{AbA}	71.89±0.06 ^{AeA}	71.43±0.14 ^{BbA}	71.35±0.32 ^{BfA}	71.34±0.07 ^{BeA}
<i>a*</i>								
NN	-0.79±0.03 ^{CdA}	-0.57±0.02 ^{AcA}	-0.57±0.02 ^{AcA}	-0.61±0.02 ^{BeA}	17.65±0.09 ^{BcA}	17.70±0.10 ^{BbA}	18.13±0.12 ^{AbA}	18.14±0.04 ^{AdA}
NG	-0.83±0.02 ^{BdA}	-0.62±0.02 ^{AcA}	-0.68±0.17 ^{AcD}	-0.66±0.01 ^{AeA}	18.27±0.10 ^{DbA}	18.65±0.11 ^{CaA}	18.82±0.14 ^{BaA}	18.97±0.06 ^{AbA}
GN	-0.83±0.01 ^{CdA}	-0.78±0.02 ^{BdA}	-0.67±0.02 ^{AcD}	-0.67±0.03 ^{AeA}	18.31±0.24 ^{BbA}	18.70±0.27 ^{AaA}	18.81±0.11 ^{AaA}	18.74±0.06 ^{AcA}
GG	-0.81±0.02 ^{BdA}	-0.79±0.01 ^{BdA}	-0.77±0.14 ^{BdA}	-0.66±0.02 ^{AeA}	18.53±0.18 ^{CaA}	18.68±0.11 ^{BCa}	18.85±0.20 ^{BaA}	19.30±0.12 ^{AaA}
<i>b*</i>								
NN	2.70±0.03 ^{BfA}	2.69±0.04 ^{BeA}	2.75±0.11 ^{BdA}	2.94±0.03 ^{AfA}	50.21±0.19 ^{DcA}	50.62±0.18 ^{CcA}	51.37±0.08 ^{BbA}	51.75±0.10 ^{AcA}
NG	3.08±0.05 ^{BeA}	3.45±0.05 ^{AdA}	3.36±0.44 ^{ABc}	3.51±0.04 ^{AeA}	51.43±0.14 ^{CaA}	52.20±0.29 ^{BaA}	52.47±0.19 ^{BaA}	52.96±0.25 ^{AaA}
GN	3.19±0.03 ^{BeA}	3.57±0.04 ^{AdA}	3.22±0.22 ^{BcA}	3.46±0.03 ^{AeA}	50.91±0.15 ^{CbA}	51.99±0.24 ^{BbA}	52.38±0.05 ^{AaA}	52.27±0.05 ^{AbA}
GG	3.50±0.02 ^{AdA}	3.58±0.02 ^{AdA}	3.46±0.45 ^{AcA}	3.67±0.03 ^{AdA}	51.26±0.25 ^{CaA}	51.96±0.13 ^{BbA}	52.19±0.21 ^{BaA}	52.95±0.17 ^{AaA}

NN, double emulsion without gallic acid; GN, double emulsion containing gallic acid in the W₁ phase; NG, double emulsion containing gallic acid in the W₂ phase; GG, double emulsion containing gallic acid in both W₁ and W₂ phases. Different lowercase

letters within the same column and uppercase letters within the same row indicate significant differences ($p < 0.05$) according to Duncan's multiple range test following a one-way ANOVA.

ARTICLE IN PRESS

Table 3 Carotenoids content of double emulsions containing 0.5% paprika oleoresin in the oil phase with different compositions and storage periods

Treatment	Storage time (weeks)			
	0	1	2	4
Red isochromatic fraction (mg carotenoids/g sample), C^R				
NN	1.70±0.05 ^{Ab}	1.58±0.02 ^{Ba}	1.28±0.03 ^{Ca}	1.20±0.06 ^{Db}
NG	1.75±0.02 ^{Aa}	1.58±0.02 ^{Ba}	1.33±0.03 ^{Ca}	1.24±0.01 ^{Da}
GN	1.76±0.03 ^{Aa}	1.57±0.02 ^{Ba}	1.26±0.04 ^{Ca}	1.22±0.02 ^{Dab}
GG	1.75±0.03 ^{Aa}	1.58±0.01 ^{Ba}	1.27±0.04 ^{Ca}	1.22±0.02 ^{Dab}
Yellow isochromatic fraction (mg carotenoids/g sample), C^Y				
NN	1.54±0.08 ^{Ab}	1.35±0.03 ^{Bb}	1.09±0.03 ^{Ca}	0.97±0.07 ^{Db}
NG	1.56±0.03 ^{Aa}	1.37±0.03 ^{Bb}	1.08±0.03 ^{Ca}	1.05±0.02 ^{Da}
GN	1.54±0.06 ^{Aa}	1.40±0.02 ^{Ba}	1.11±0.04 ^{Ca}	1.05±0.01 ^{Da}
GG	1.56±0.04 ^{Aa}	1.41±0.02 ^{Ba}	1.11±0.04 ^{Ca}	1.04±0.01 ^{Da}
Total carotenoid content (mg carotenoids/g sample), C^T				
NN	3.24±0.02 ^{Ab}	2.93±0.04 ^{Bb}	2.37±0.06 ^{Ca}	2.16±0.03 ^{Db}
NG	3.31±0.02 ^{Aa}	2.94±0.04 ^{Bb}	2.41±0.06 ^{Ca}	2.29±0.03 ^{Da}
GN	3.30±0.03 ^{Aa}	2.97±0.02 ^{Bab}	2.38±0.08 ^{Ca}	2.27±0.02 ^{Da}
GG	3.31±0.01 ^{Aa}	2.99±0.02 ^{Ba}	2.39±0.08 ^{Ca}	2.26±0.02 ^{Da}

NN, double emulsion without gallic acid; GN, double emulsion containing gallic acid in the W_1 phase; NG, double emulsion containing gallic acid in the W_2 phase; GG, double emulsion containing gallic acid in both W_1 and W_2 phases. Different lowercase letters within the same column and uppercase letters within the same row indicate significant differences ($p < 0.05$) according to Duncan's multiple range test following one-way ANOVA.